Instanton content of finite temperature QCD matter

M.-C. Chu[1] and S. Schramm[2,3]

[1] *W. K. Kellogg Radiation Laboratory, 106-38,*

California Institute of Technology, Pasadena, California 91125

[2] *Nuclear Theory Center, Indiana University, Bloomington, Indiana 47408*

[3] *GSI, 64220 Darmstadt, Germany*

(February 9, 2008)

Abstract

We investigate the temperature dependence of the instanton content of gluon fields and their contribution to quark correlation using quenched lattice QCD and the cooling method. We found a suppression of the topological susceptibility at finite temperature, agreeing with the PCAC expectation at low temperature and enhanced suppression for temperatures at and above the deconfinement transition. For temperatures up to about 334 MeV, the topological charge correlation agrees well with a single instanton profile, though the size parameter seems to change across the phase transition. The screening wave functions for the pion and the rho become slightly more compact at higher temperatures. Lattice cooling shows no contribution from the instantons to the screening wave functions at temperatures above the phase transition.

PACS numbers: 12.38.Gc, 11.10.Wx, 12.38.Mh

I. INTRODUCTION

Lattice QCD calculations [1] have suggested the existence of a deconfinement phase transition at a critical temperature T_c, at which quark and gluons are deconfined and form a new phase of matter, the so-called *quark-gluon plasma*. This possibility stimulated numerous theoretical and phenomenological works on the subject, many of which focus on the possible experimental signatures of the quark-gluon plasma [2]. Whereas these works are extremely useful, in view of the experiments at AGS, CERN, and RHIC, theoretical studies of the properties of finite temperature QCD matter should also be important. Lattice gauge theory provides a useful tool to calculate various hadronic matrix elements from first principle, and it therefore enables us to study static finite temperature properties of QCD matter.

A particularly important and interesting question regarding QCD matter at finite temperature is what happens to the hadrons. Most of the phenomenological works on quark-gluon plasma signatures to date are based on a picture of weakly interacting quarks and gluons at temperatures above T_c. However, such a simple picture is not completely supported by lattice calculations. For example, lattice calculations of the so-called screening wave functions indicated strong correlations among the quarks in hadronic channels [3]. However, it is still an open question whether the screening wave function results have any direct bearing on the structure of hadrons at finite temperature.

In lack of a method to calculate the finite-temperature hadron wave functions directly, we turn our attention to a class of gauge configurations known to have important effects on the structure and masses of light hadrons at zero temperature [4], namely, large, isolated instantons. The primary goal of this paper is to study the instanton content of QCD matter and their contribution to quark correlations at finite temperature.

It is well known that instantons break the $U_A(1)$ chiral symmetry, resulting in the famous axial anomalies. At high temperature, Debye screening gives rise to an electric mass for the gluons and thereby suppresses instanton amplitudes; the $U_A(1)$ symmetry should therefore be restored. Whether the $U_A(1)$ restoration at T_U occurs at the same temperature as the $SU(N_f)_A$ restoration at T_c bears important consequences to the hadronic physics at finite temperature: if $T_U = T_c$, the phase transition is of first order [5] and there are drastic changes to hadrons at T_c; if, on the other hand, $T_U > T_c$, the phase transition is of second order. The two scenarios give rise to very different hadron physics at temperatures around T_c [6]. One of our goals is to locate T_U via lattice calculation of the topological susceptibility, which is a measure of the instanton content, and thereby differentiate the two scenarios.

There have been calculations of the temperature dependence of the topological susceptibility in pure SU(2) [7,8], pure SU(3) [9], as well as unquenched SU(3) with two light quark flavors [10]. However, these authors vary the temperature by adjusting the coupling constant, making it tricky to compare the susceptibility at different temperatures because of the different lattice length scales. At larger β finite size effects may plague the calculations using small (e.g., $8^3 \times 4$) lattices. There is also some confusion on the behavior of the susceptibility in the SU(2) theory. Whereas Teper *et al.* observed a sudden suppression of the topological susceptibility at the deconfinement temperature for both SU(2) and SU(3) fields [7,9], Di Giacomo *et al.* reported that the cooling method gave ambiguous results for SU(2) theory, and the susceptibility determined by their field theoretical method stays almost constant across the phase transition [8].

In this paper, we present calculations of the temperature dependence of the instanton content of quenched SU(3) fields using the cooling method. We vary the temperature by changing the number of time slices and report results for $N_t = 4$, 6, 8, 10, 12, 14, 16, $N_s = 16$, and $\beta = 6$ lattices. We did not observe the ambiguity reported for the SU(2) calculation, and the topological susceptibility is very stable with respect to the number of cooling steps. We found a suppression of the topological susceptibility starting at temperatures below T_c. The topological charge correlation function agrees well with the continuum instanton profile, although there seems to be a change in the instanton size parameter across the phase transition. For three temperatures around T_c, we also calculate the spatially-propagated wave functions, or the so-called screening wave functions, for the pion and the rho with and without cooling. We found that while the uncooled screening wave functions are only mildly sensitive to temperature, in agreement with previous calculations [3], the cooled wave functions for $T > 200$ MeV are indistinguishable from the free ones. We thus conclude that at such high temperatures, instantons do not contribute to the screening wave functions.

We first describe in Sec. II the set of observables we calculated. A brief outline of the cooling method is presented in Sec. III, and our main results are summarized in Sec. IV. We then close with some discussions in Sec. V.

II. OBSERVABLES

The instanton content of the gauge fields can be monitored by the the topological charge density, which can be defined on the lattice as

$$Q(x_n) = -\frac{1}{32\pi^2}\epsilon_{\alpha\beta\gamma\delta}\mathrm{Re\ Tr}\left[U_{\alpha\beta}(x_n)U_{\gamma\delta}(x_n)\right] \ , \tag{1}$$

where $U_{\alpha\beta}$ is the product of the link variables around a plaquette in the $\alpha - \beta$ plane, after some cooling steps were applied to remove lattice artifacts associated with discretization [9]. The topological susceptibility is then given as the fluctuations of the topological charge:

$$\chi_t \equiv \frac{1}{N_t N_s^3 a^4}\langle\left(\sum_n Q(x_n)\right)^2\rangle \ , \tag{2}$$

where $\langle\ldots\rangle$ indicates configuration averaging, and N_t and N_s are the number of sites in the temporal and spatial direction. The lattice spacing a changes as a function of the lattice inverse coupling β, which makes it tricky to compare χ_t calculated with different β, especially when β is not large enough to be in the asymptotic scaling regime. To study the temperature dependence of the topological susceptibility, we chose to change the temperature by varying the number of time slices

$$T = \frac{1}{N_t a} \ , \tag{3}$$

but keeping fixed β and hence a. This way the uncertainty in a enters only as an overall constant factor which does not affect the shape of the χ_t vs. T curve.

In order to look into the details of the topological charge distribution, we also calculated the topological charge density correlation function [4]

$$C_Q(x) = \langle \sum_y Q(y)Q(x+y)\rangle / \langle \sum_y Q^2(y)\rangle \ . \tag{4}$$

One can compare this correlation function to a convolution of an isolated instanton topological charge density

$$Q_\rho(x) = \frac{6}{\pi^2\rho^4}\left(\frac{\rho^2}{x^2+\rho^2}\right)^4 \ , \tag{5}$$

where ρ is the size parameter. Zero temperature calculations using the cooling method [4] show that after about 50 cooling steps, the gauge fields are dominated by large, isolated instantons, whose profiles agree well with that given by the continuum analytic expression Eq. (5) with $\rho \approx 0.3$ fm. We will monitor the temperature dependence of the topological charge density correlation as given by Eq. (4).

At zero temperature, due to Euclidean symmetry the space-like and time-like plaquettes (P_x, P_t) have equal expectation values. At finite temperature, however, the Euclidean symmetry is broken, and an asymmetry between the space-like and time-like plaquettes develops at the phase transition temperature proportional to the entropy s of the system [11]:

$$Ts = \epsilon + P = 4\beta\left[1 - 0.16675g^2 + O(g^4)\right](\langle P_t\rangle - \langle P_x\rangle) \ , \tag{6}$$

where

$$\langle P_t\rangle \equiv \frac{1}{3N_s^3N_t}\sum_{n,i}\frac{1}{3}\mathrm{Tr}U_{0,i}(x_n) \ , \tag{7}$$

and

$$\langle P_x\rangle \equiv \frac{1}{3N_s^3N_t}\sum_{n,i<j}\frac{1}{3}\mathrm{Tr}U_{i,j}(x_n) \ . \tag{8}$$

Since the pressure p is continuous across the phase transition, the discontinuity of $\epsilon + p$ is the latent heat $\Delta\epsilon$. Understanding the physics origin of the latent heat is important to developing models for finite temperature hadronic matter. For example, it was postulated in Ref. [12] that instanton liquid reorganizes into molecules near T_c and this process contributes to a jump in the energy density at T_c. Here we calculate the latent heat from both cooled and uncooled configurations so as to monitor the contribution of the instantons to this quantity.

To study the quark distribution in various hadronic channels, we calculate the Bethe-Salpeter amplitudes [3,13]:

$$\Psi_\pi^{\mathrm{BS}}(y) \equiv \int d\vec{x}\langle\Omega|\bar{d}(\vec{x})P\, e^{\,i\int_{\vec{x}}^{\vec{x}+\vec{y}} A(\vec{x}')d\vec{x}'}\gamma_5 u(\vec{x}+\vec{y})|\pi\rangle \tag{9}$$

$$\Psi_\rho^{\mathrm{BS}}(y) \equiv \int d\vec{x}\langle\Omega|\bar{d}(\vec{x})P\, e^{\,i\int_{\vec{x}}^{\vec{x}+\vec{y}} A(\vec{x}')d\vec{x}'}\gamma_2 u(\vec{x}+\vec{y})|\pi\rangle \ . \tag{10}$$

Here, $|\Omega\rangle$ is the vacuum state, and P indicates path-ordering of the gauge fields A put in to make the amplitudes gauge invariant. We have used the natural choice of a straight line

joining the two quarks at $\vec{x}$ and $\vec{x}+\vec{y}$. When T is finite, the above amplitudes are extracted at large z instead of the usual Euclidean time filtering. This results in a projection into the lowest *momentum* state, and therefore one cannot interpret the resulting amplitudes as a *wavefunction*. However, some insights into hadronic structure can be obtained by comparing the QCD calculations to model results [3,14,15]. In particular, one can compare the amplitudes for free quarks with those calculated at various temperatures, to check whether at some temperature, hadronic matter behaves like weakly interacting quark-gluon gas. Such a comparison has been done in two recent papers [3], with the surprising result that the Bethe-Salpeter amplitudes seems to be quite insensitive to changes in temperature up to $T = 1.5T_c$. In this paper, we extend the previous calculations to higher temperature $T = 2T_c$, and we also calculate the amplitudes from cooled configurations so that we can correlate any changes in the amplitudes with the instanton content of the gauge fields.

III. COOLING

The method of lattice cooling has been extensively studied and discussed in the literature [9]. The method can be applied to finite temperature configurations without modifications. We used the same procedure as in Ref. [4].

Briefly speaking, the cooling method smooths out the gauge fields locally, by minimizing the action density. After some cooling steps the short-range fluctuations in the gauge fields are suppressed, leaving the long-range "bumps" more or less unchanged. In particular, large isolated instantons, which are protected by topology, dominate the gauge fields after many cooling steps, while the smaller instantons annihilate with nearby anti-instantons. The topological charge approaches a plateau corresponding to an integral number of instantons when plotted against the number of cooling steps. The topological susceptibility then becomes constant, since the annihilation of instanton pairs does not change its value. Only then can one extract an unambiguous value for the susceptibility using the cooling method. In Fig. 1 we show the cooling history of $\langle Q^2 \rangle$ for several N_t. In contrast to Ref. [8], we have no problem extracting $\langle Q^2 \rangle$ and therefore the susceptibility even for $T > T_c$.

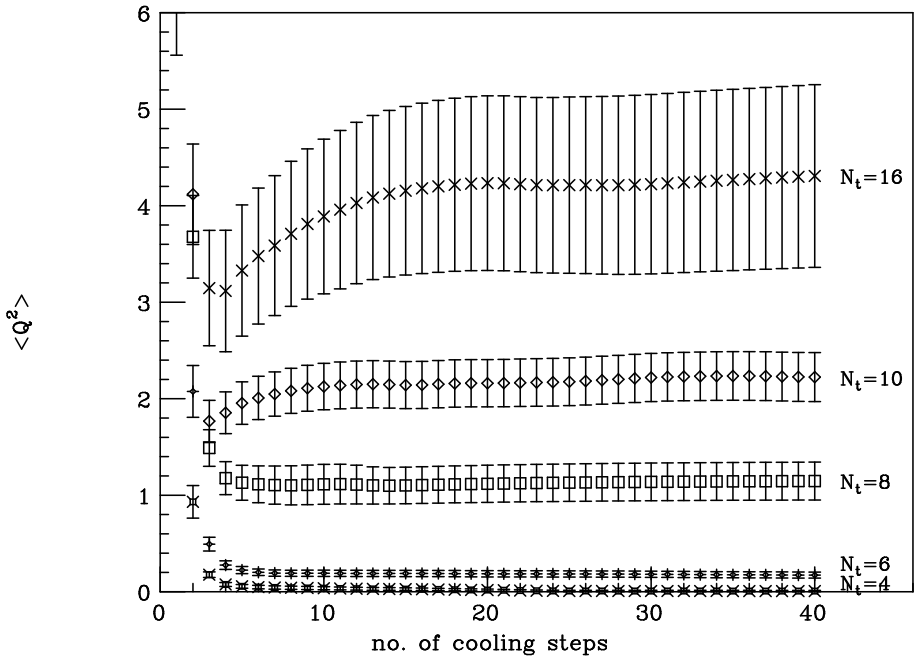

FIG. 1. The expectation value of topological charge squared vs. number of cooling steps for $N_t = 4$, 6, 8, 10, and 16. The quenched configurations are generated using $\beta = 6$ and $N_s = 16$. In all cases, the values of $\langle Q^2 \rangle$ become unchanged after only about 15 cooling steps. Same behavior was found for $N_t = 12$ and 14 as well, though not shown here for clarity. The error bars reflect statistical uncertainties in the configuration averaging only.

After many cooling steps, the instantons are well separated in the gauge fields, and the dilute gas approximation should become valid. The probability distributions for topological charge is then given by a convolution of Poissonian distributions [9]:

$$P(Q) = e^{-2m} m^Q \sum_{i=0}^{\infty} \frac{m^{2i}}{i!(i+Q)!} \, , \tag{11}$$

and the dilute gas value of $\langle Q^2 \rangle$ is then given by

$$\langle Q^2 \rangle = 2m \, . \tag{12}$$

In the case of an ideal Poissonian process, m would be equal to the number of instantons (anti-instantons). A comparison of the distribution of topological charge at various N_t with the dilute gas approximation (dashed lines) is given in Fig. 2. Their agreement gives a nontrivial check that our gauge fields are dominated by dilute instanton ensembles after our cooling procedure, and the topological susceptibility we extract from Fig. 1 reflects the fluctuations in the topological charge in the ensembles.

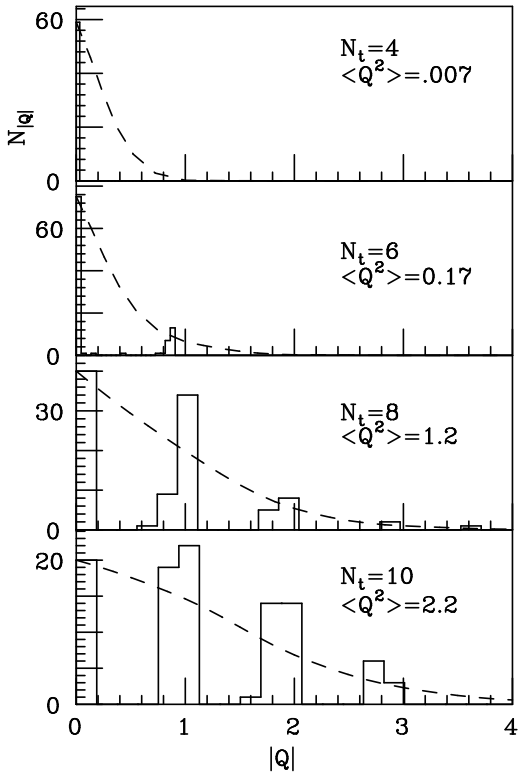

FIG. 2. Histograms showing the distribution of topological charge in the configurations for $N_t = 4$, 6, 8, and 10. The dashed lines show the distribution given by the dilute gas approximation (see Sec. III), using the $\langle Q^2 \rangle$ read from Fig. 1. Notice the clustering of data around integral values of the topological charge.

IV. RESULTS

For the generation of the gauge field configurations we used the Metropolis algorithm. We studied a lattice with spatial volume $V_s = 16^3$. Following Eq. (3), we varied the temperature by varying the number of time slices using values $N_t = 4$, 6, 8, 10, 12, 14, and 16, respectively. The coupling constant is chosen to be $\beta = 6.0$ which corresponds to a physical lattice spacing $a \sim 0.1$ fm. Thus the calculation covers a temperature range between 125 and 500 MeV. For this value of β the critical temperature is $T_c \sim 250$ MeV. We generated 100 configurations each for $N_t = 4$, 6, 8, 10, 12, and 40 configurations for $N_t = 14$ and 16, which were separated by 300 lattice sweeps. The configurations were then cooled for 40 steps using the Cabibbo-Marinari heat bath algorithm in the limit of infinite coupling strength $b = \infty$ as discussed in Ref. [4]. We verified the stability of our results by varying the number of cooling steps.

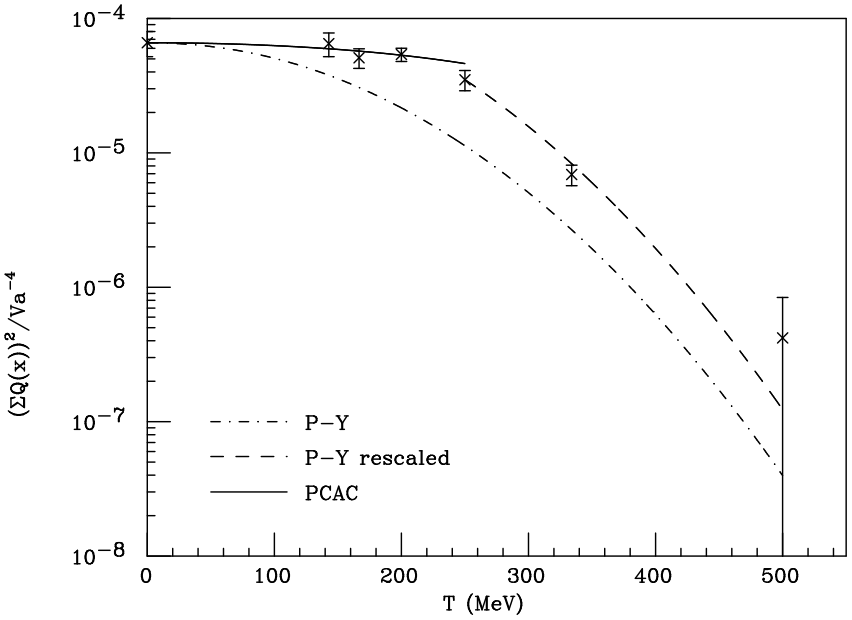

FIG. 3. Topological susceptibility as a function of temperature. Lattice data, shown with error bars, are compared with: 1) the PCAC expectation assuming soft pion gas as the heat bath, taking $c = -1/6$ and $F_\pi = 186$ MeV (see Eq. 15), indicated by the solid line; 2) the Pisarski-Yaffe formula (Eq. 16, using $\rho = 0.26$ fm), derived assuming Debye-screening mechanism of instanton suppression, indicated by the dotdashed line; 3) the Pisarski-Yaffe formula rescaled to match with the value of the topological susceptibility at $T_c = 250$ MeV, shown in dashed line. The phenomenological value is also plotted at zero temperature.

The numerical values for the topological susceptibility are shown in Fig. 3. The plot also shows the approximate phenomenological value for χ_t at zero temperature as estimated by Witten and Veneziano [16]

$$\chi_t = \frac{f_\pi^2}{4N_f}(m_{\eta'}^2 - 2m_K^2 + m_\eta^2) \sim (180 \text{ MeV})^4 \, . \tag{13}$$

As can be seen, the phenomenological value and the numerical result for the $V = 16^4$ lattice agree quite well. The temperature behavior of χ_t exhibits a gentle decrease for $T < T_c$, turning into a relatively sharp decay of the susceptibility around the critical temperature T_c. At low temperature, $T \ll T_c$, one can model the heat bath as a soft pion gas and apply PCAC methods [17] to obtain

$$\chi_t(T) = \chi_t(T = 0)\left(1 + cT^2/F_\pi^2\right) \, , \tag{14}$$

with $-1/6 \leq c \leq 1/6$. A very mild temperature dependence is thus predicted for low temperature. We show in Fig. 3 the maximum suppression of the topological susceptibility ($c = -1/6$) by the solid line, which agrees quite well with our data up to $T \approx 200$ MeV, though our statistics is not good enough to narrow down the range of a. The agreement is probably accidental though, since our quenched configurations should not reproduce the physics of a thermal pion gas. The instanton density is suppressed by a factor of one half when $T = T_c$, with some stronger suppression mechanism operative at temperatures between

$T = 200$ MeV and T_c. A rather sharp decrease of the topological susceptibility continues above the phase transition. At temperature $T \sim 334$ MeV topological effects are strongly suppressed; χ_t is practically zero at $T \sim 500$ MeV. The dotdashed curve in Fig. 3 shows the temperature dependence for χ_t as predicted by Pisarski and Yaffe [18] calculating the Debye-screening suppression of large scale instantons:

$$\chi_t(T) = \chi_t(T=0)\left(1+\lambda^2/3\right)^{\frac{3}{2}} \exp\left[-2\lambda^2 - 18\alpha\left(1+\gamma\lambda^{\frac{-3}{2}}\right)^{-8}\right] , \tag{15}$$

for quenched $SU(3)$ fields, with $\lambda \equiv \pi\rho T$, $\alpha = 0.01289764$, $\gamma = 0.15858$, and $\rho = 0.26$ fm is the size parameter of instantons we obtained by fitting our $N_t = 6$ data (see discussion below), which differs slightly from a previous lattice calculation at zero temperature [4]. The perturbative result in Eq. 15 is supposed to be valid only at very high temperature. In the temperature range we are considering, the perturbative formula gives too large a suppression. The dashed curve in Fig. 3 was computed by rescaling the Pisarski-Yaffe expression to match with the susceptibility at $T_c = 250$ MeV, which then seems to be in agreement with the data, though more data is needed between T_c and $2T_c$ for a more meaningful comparison. The phenomenological consequences of the restoration of $U_A(1)$, such as changes in the η' mass, should be an exciting subject for experimental works at AGS, CERN, and RHIC.

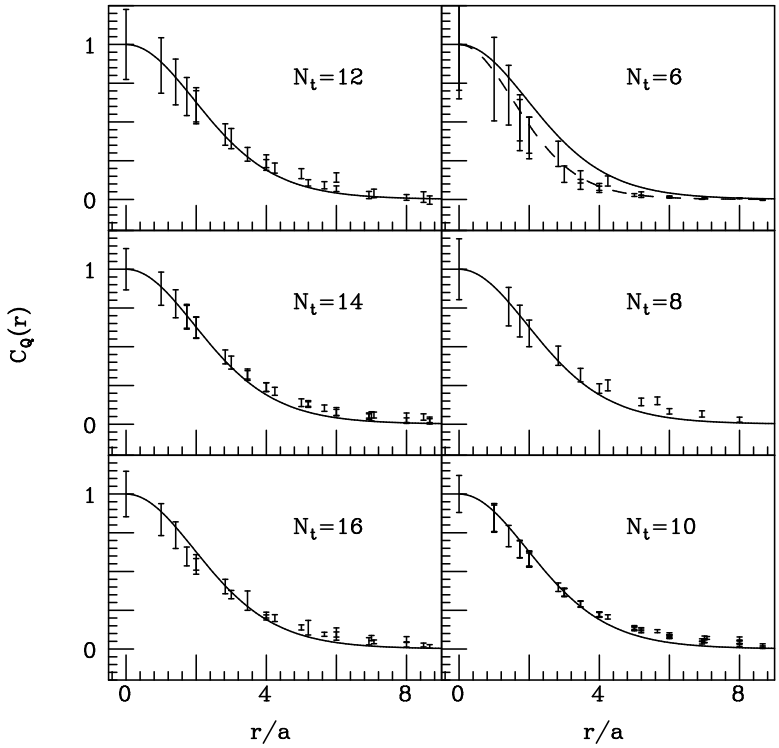

FIG. 4. Topological charge correlation function, calculated for $N_t = 6$, 8, 10, 12, 14, and 16. The solid lines show the correlation function calculated with the continuum instanton charge distribution assuming a size parameter $\rho = 3.3a$. The dashed line shown at $N_t = 6$ is the continuum instanton correlation function with $\rho = 2.6a$.

In Fig. 4 we show the correlation function $C_Q(x)$, Eq. (4), with x taken in the spatial direction. Six different temperatures are shown. For comparison the plots include the

correlation function calculated with an isolated instanton with size parameter $\rho = 3.3a \sim 0.33$ fm, which fits the data reasonably well for all temperatures up to T_c, at $N_t = 8$. At $T \approx 334$ MeV, or $N_t = 6$, the instanton profile with $\rho = 2.6a \sim 0.26$ fm gives a better fit to the data. In Fig. 5, we show the cooling dependence of the topological charge correlation function for $N_t = 6$. The shape of the correlation is very stable between 20 and 100 cooling steps, and the smaller size parameter $\rho = 0.26$ fm is clearly favored by the data over the larger one ($\rho = 0.33$ fm) preferred at lower temperatures. As can be seen, the temperature dependence is quite weak below T_c, but our data suggests a rather sudden change in ρ across the phase transition. This may signal major reorganization in the gluon fields above T_c. For $N_t = 4$, the topological charge correlation function changes continuously as a function of cooling steps, and therefore we could not extract a meaningful shape at that temperature. The correlation function becomes flat at small N_t when x is taken in the temporal direction because of the periodic boundary condition.

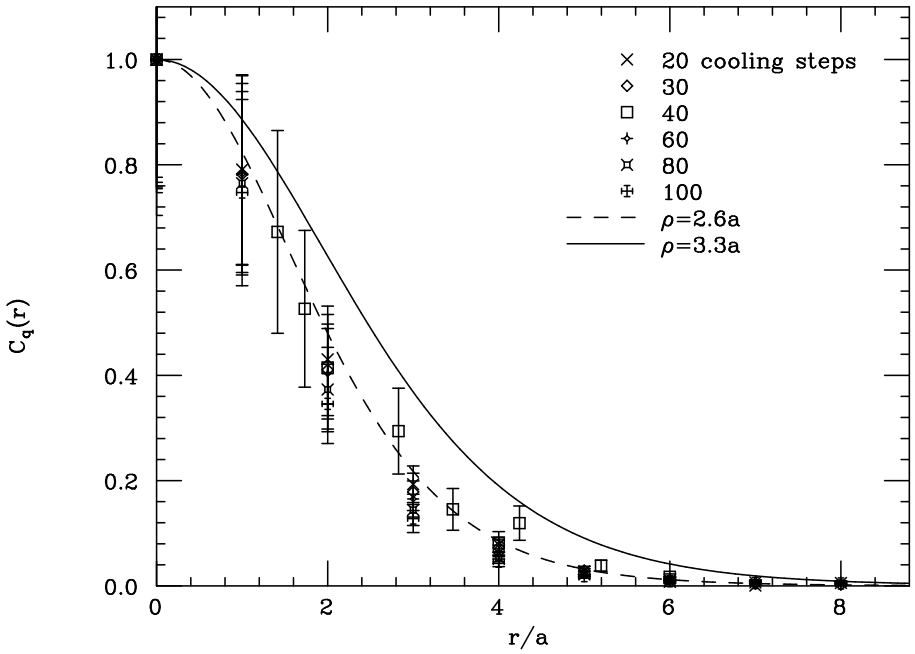

FIG. 5. Topological charge correlation function for $N_t = 6$, at different cooling steps. The solid and dashed lines are the same as in Fig. 4.

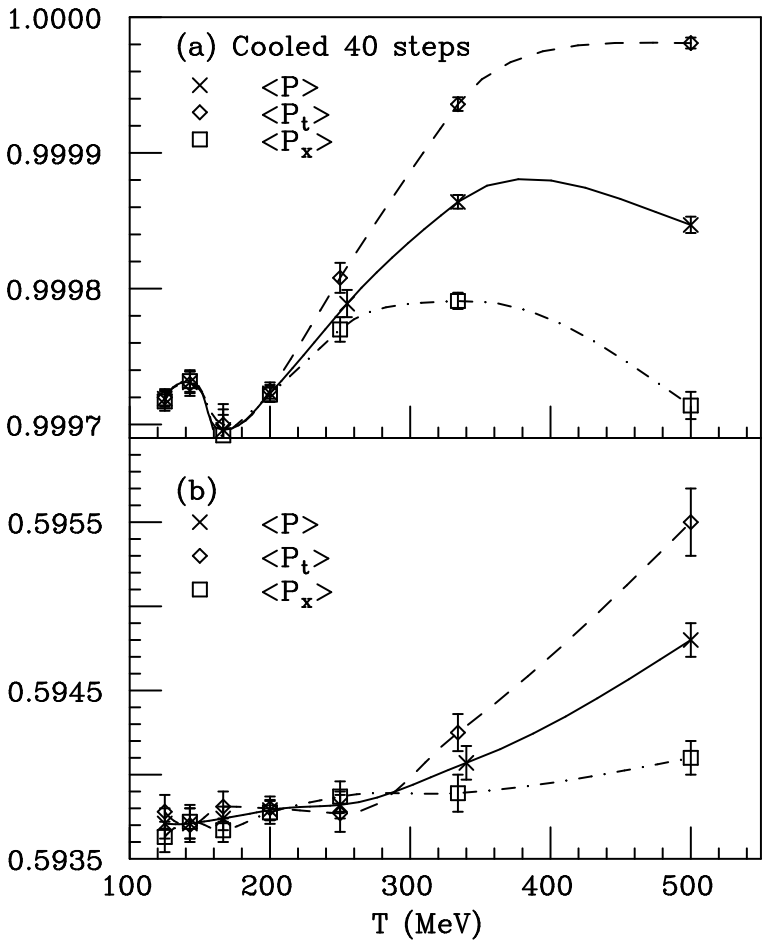

FIG. 6. Plaquette expectation values as a function of temperature for (a) cooled and (b) uncooled configurations. The space-like plaquette expectation values $\langle P_x \rangle$ (squares) are compared to the time-like ones $\langle P_t \rangle$ (diamonds) and the overall averages $\langle P \rangle$ (crosses). The lines are drawn to guide the eyes only.

We monitor the contribution of the large, isolated instantons to the latent heat by calculating the splittings of the spatial and temporal plaquettes for both cooled and uncooled configurations. The numerical values of the plaquettes are plotted in Fig. 6 (a) and (b), where a clear splitting between the spatial and temporal plaquettes, $\Delta P \equiv \langle P_t \rangle - \langle P_x \rangle$, can be seen for temperatures above the phase transition. The splitting ΔP, which is proportional to the latent heat, is clearly a function of cooling, and it approaches zero in the limit of infinite cooling steps. An estimate of the fraction of latent heat contributed by instantons, f, is given by

$$f \approx \frac{\Delta P_{\rm cooled}}{\Delta P_{\rm uncooled}} \, . \tag{16}$$

In Fig. 7 we show f as a function of cooling steps for both $N_t = 4$ and 6. In both cases, f drops very quickly in the first 40 cooling steps, showing that most of the splitting is due to short range fluctuations that got eliminated by cooling. After about 50 cooling steps, the $N_t = 4$ splitting levels off to a plateau, where its value represents an upper bound to the

contribution of the instantons at $T = 500$ MeV. The splitting at $N_t = 6$ has not reached a plateau yet even at 100 cooling steps; we quote just the fraction f at 100th cooling step as the upper bound at $T = 334$ MeV. Our results for f are 0.15 ± 0.04 at $T = 334$ MeV and 0.056 ± 0.004 at $T = 500$ MeV.

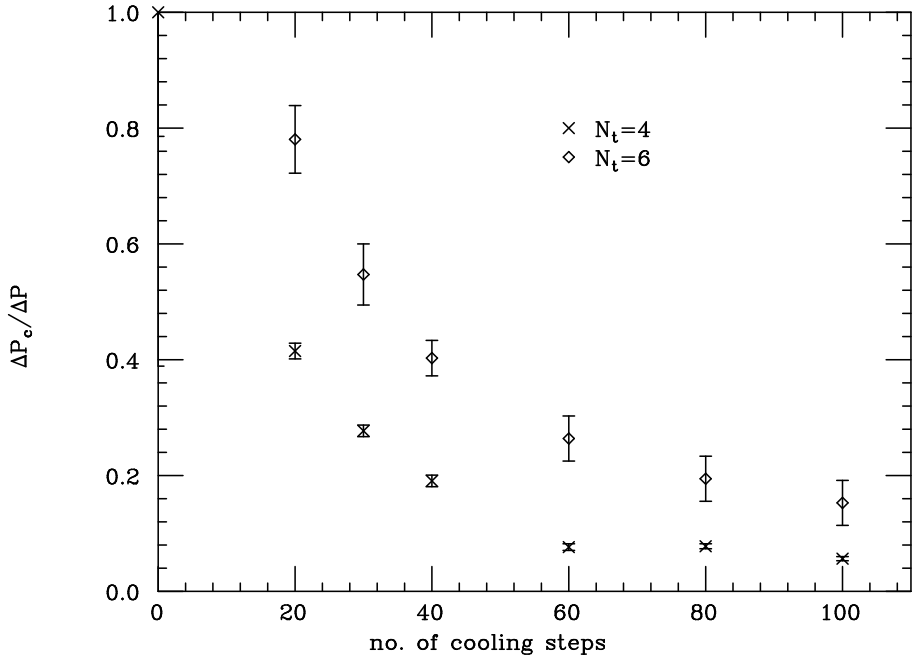

FIG. 7. Plaquette splittings, $\Delta P_c = \langle P_t \rangle - \langle P_x \rangle$, normalized to their uncooled values, as a function of cooling steps. $N_t = 4$ data are shown as crosses, and $N_t = 6$ data as diamonds. Values at 100th cooling step represent upper bounds to the fraction of latent heat contributed by the instantons.

Finally, we computed the screening wave functions for the π and ρ mesons as explained in Sec. II. We used a conjugate gradient procedure to calculate the Greens functions for Wilson fermions with $\kappa = 0.1541$, which corresponds to a quark mass $m \sim 100$ MeV. The average of a set of ten wave functions for $N_t = 10, 6, 4$ corresponding to $T = 200, 334, 500$ MeV are shown in Figs. 8 and 9. As already observed in [3] the screening wave functions change only slightly as a function of temperature across T_c. The spatial extension of the wave functions shrinks as temperature increases, in agreement with theoretical arguments discussed in Refs. [3,14]. Here the main idea is that in the deconfined phase, the quark mass for propagation along the spatial axis is essentially given by the lowest Matsubara frequency $m \sim \pi T$. Strong correlations resulting from unscreened magnetic interactions generate a bound state between quarks propagating along a spatial axis even in the deconfined phase. The effective quark mass increases at high temperatures, thus decreasing the characteristic size of the state. However, the weak dependence of the wave functions is surprising in view of the factor of 2.5 increase in the effective quark mass from $N_t = 10$ to 4. It is probable that the present temperature range is not high enough for the above picture based on dimensional reduction to be accurate.

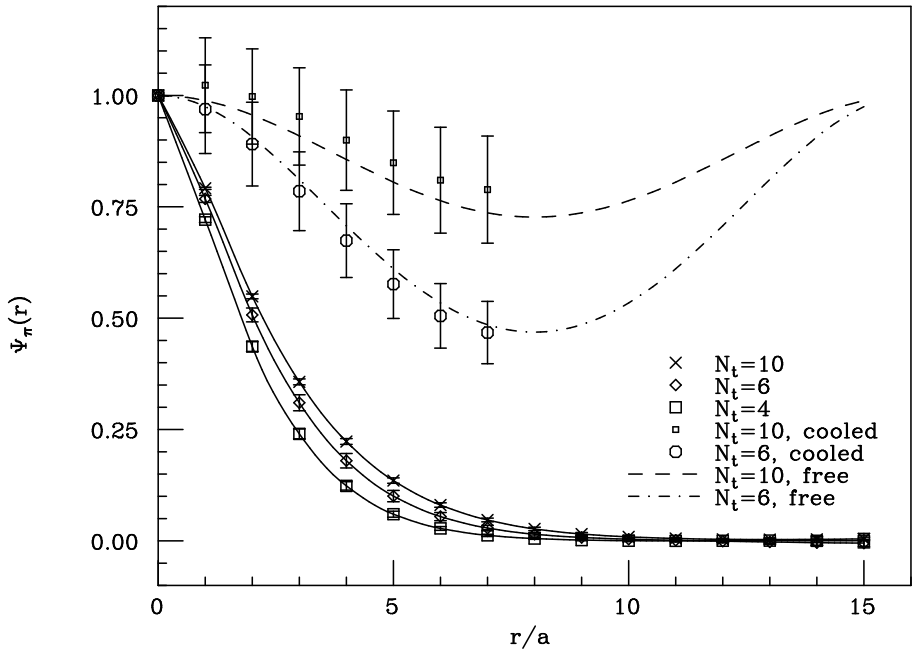

FIG. 8. Screening wave functions of the π meson, for $N_t = 4$ (squares), 6 (diamonds), and 10 (crosses), corresponding to $T = 500$, 334, 200 MeV, respectively. wave functions calculated with cooled configurations and symmetrized to take into account of the periodic boundary conditions are also shown for $N_t = 6$ (circles) and 10 (small squares), which agree well with free wave functions (dashed and solid lines).

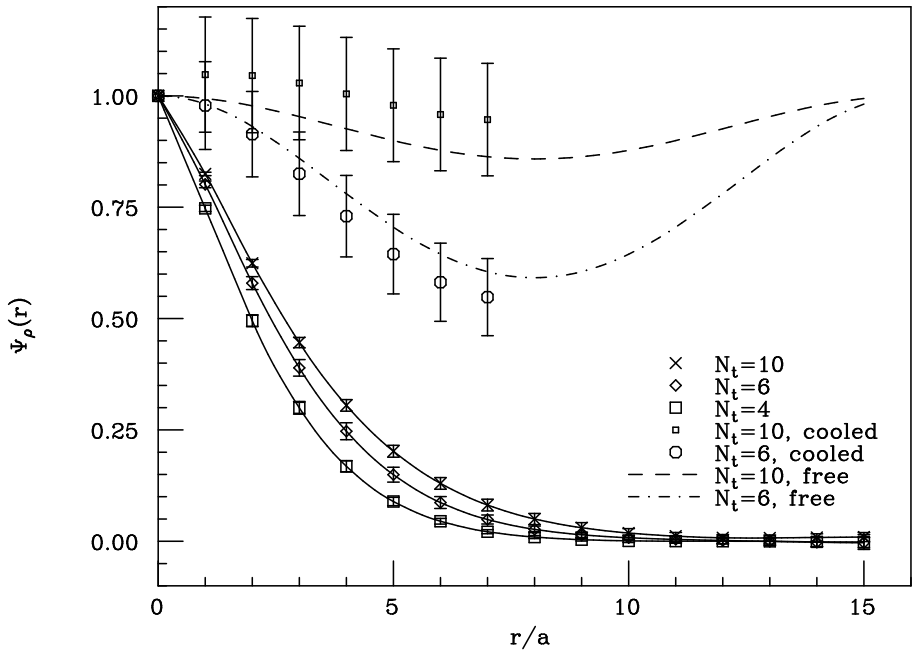

FIG. 9. Screening wave functions of the ρ meson, see Fig. 8.

As in the case of zero temperature, cooling effectively removed short range fluctuations in the gauge fields responsible for quark confinement as well as the Coulomb force. As a result, the wave functions calculated from the cooled configurations are distinctly broader, with the slope at short distances strongly reduced [4]. To study the contribution of instantons to the screening wave functions at such high temperatures, we compare the cooled wave functions with the uncooled ones as well as the free wave functions. As shown in Figs. 8 and 9, for both π and ρ at $T = 200$ and 500 MeV, after symmetrized to take into account the periodic boundary conditions, the cooled wave functions are indistinguishable from the free ones. Our results imply that the large scale instantons do not play an important role in the screening wave functions in this range of the temperature. This is possibly a result of both the suppression of instanton density and the increase of the effective quark mass by the Matsubara frequency. Instead, some non-trivial interactions are operative, which correlate the effective massive quarks. It is important to understand this mechanism in order to develop an accurate phenomenology of hadronic physics at temperatures around T_c, just where the current and future heavy-ion experiments probe.

V. SUMMARY

We discussed the content and the role of instantons in quenched QCD matter at finite temperature. Specifically, we calculated the density of instantons and found that it is suppressed as temperature increases. While the mild dependence of χ_t can be understood by a PCAC method assuming a soft pion gas as the heat bath, the high temperature ($T > T_c$) behavior deviates significantly from the perturbative formula expressing the Debye-screening suppression of instantons. Our results indicate that the restoration of $U_A(1)$ symmetry is a continuous process starting below T_c; at T_c, about half of the axial anomalies are already removed. Some non-perturbative mechanism enhances the rate of $U_A(1)$-restoration in the temperature range $T_c \leq T \leq 2T_c$. The topological charge correlation function agrees well with the continuum instanton profile, though our data suggests a rapid change in the size parameter from $\rho = 0.33$ fm at and below 250 MeV to 0.26 fm at 334 MeV. By comparing the entropy in the cooled and uncooled gauge fields, we obtain upper bounds — of about 5% at $2T_c$ and 15% at $1.5T_c$ — on the instanton contribution to the latent heat. The screening wave functions of π and ρ mesons show a weak temperature dependence for temperatures as high as $2T_c$. This points to strong correlations between quarks even in the deconfined phase. In contrast to the zero temperature situation, the screening wave functions at temperatures above $T \approx 200$ MeV are not dominated by the instantons.

It will be interesting to compare these results with unquenched calculations, as it is quite possible that the reorganization of the gauge fields near the phase transition is sensitive to the presence of dynamical quarks. Much more theoretical work is needed to illuminate the complex and drastic changes of hadronic physics near the phase transition.

We thank Suzhou Huang and Edward Shuryak for stimulating discussions. We thank the San Diego Supercomputer Center as well as the National Energy Research Supercomputer Center for providing Cray-C90 computer resources. This research is supported in part by the National Science Foundation, Grant Nos. PHY90-13248 and PHY94-12818, at Caltech and the U.S. Department of Energy, Grant No. DE-FG02-87ER40365, at Indiana University.

REFERENCES

[1] L. D. McLerran and B. Svetitsky, Phys. Lett. **98B**, 195 (1981); J. Kuti, J. Polónyi, and K. Szlachányi, Phys. Lett. **98B**, 199 (1981); J. Engels, F. Karsch, H. Satz, and I. Montvay, Phys. Lett. **101B**, 89 (1981).

[2] See for example, Nucl. Phys. **A566**, 115c (1994), and references therein.

[3] C. Bernard *et al.*, Phys. Rev. Lett. **68**, 2125 (1992); S. Schramm and M.-C. Chu, Phys. Rev. D **48**, 2279 (1993).

[4] M.-C. Chu, J. M. Grandy, S. Huang, and J. W. Negele, Phys. Rev. D **49**, 6039 (1994); Phys. Rev. Lett. **70**, 225 (1993); M.-C. Chu and S. Huang, Phys. Rev. D **45**, 2446 (1992).

[5] R. D. Pisarski and F. Wilczek, Phys. Rev. D **29**, 338 (1984).

[6] E. Shuryak, Comm. Nucl. Part. Phys. **21**, 235 (1994).

[7] M. Teper, Phys. Lett. **B171**, 81 (1986).

[8] A. DiGiacomo, E. Meggiolaro, and H. Panagopoulos, Phys. Lett. **B277**, 491 (1992).

[9] J. Hoek, M. Teper, and J. Waterhouse, Nucl. Phys. **B288**, 589 (1987).

[10] Steven Gottlieb *et al.*, Phys. Rev. D **47**, 3619 (1993).

[11] J. Engels, F. Karsch, H. Satz, and I. Montvay, Nucl. Phys. **B205**, 545 (1982); F. Brown *et al.*, Phys. Rev. Lett. **61**, 2058 (1988).

[12] E. M. Ilgenfritz and E. Shuryak, Phys. Lett. **B325**, 263 (1994); T. Schäfer, E. Shuryak, and J. J. M. Verbaarschot, Report No. SUNY-NTG-93-39 (unpublished).

[13] B. Velikson and D. Weingarten, Nucl. Phys. **B249**, 433 (1985); S. Gottlieb, in *International Conference on Advances in Lattice Gauge Theory*, Tallahassee, 1985, edited by Duke and Owens (World Scientific, Singapore, 1985) p. 105; M.-C. Chu, M. Lissia, and J. W. Negele, Nucl. Phys. **B360**, 31 (1991).

[14] V. Koch, E. V. Shuryak, G. E. Brown, A. D. Jackson, Phys. Rev. D **46**, 3169 (1992); Phys. Rev. D **47**, 2157 (1992).

[15] T. Schäfer and E. V. Shuryak, Phys. Rev. D**50**, 478 (1994).

[16] E. Witten, Nucl. Phys. **B156**, 269 (1979); G. Veneziano, Nucl. Phys. **B156**, 213 (1979); Phys. Lett. **95B**, 90 (1980).

[17] E. Shuryak and M. Velkovsky, Phys. Rev. D **50**, 3323 (1994).

[18] R. D. Pisarski and L. G. Yaffe, Phys. Lett. **B97**, 110 (1980).